ELSEVIER

Earth and Planetary Science Letters 189 (2001) 141–153

EPSL

www.elsevier.com/locate/epsl

Seismic evidence for a thermo-chemical boundary at the base of the Earth's mantle

Lianxing Wen [a,*], Paul Silver [b], David James [b], Randy Kuehnel [b]

[a] *Department of Geosciences, State University of New York at Stony Brook, Stony Brook, NY, USA*
[b] *Department of Terrestrial Magnetism, Carnegie Institution of Washington, Washington, DC, USA*

Received 23 February 2001; received in revised form 2 May 2001; accepted 2 May 2001

Abstract

We report seismic evidence for a unique 300 km thick layer at the base of the mantle beneath the south Atlantic ocean, with a steeply dipping edge, anomalously low shear wave velocities linearly decreasing from 2% (top) to 10–12% (bottom), and a maximum P velocity decrease of 3% relative to the preliminary reference Earth model (PREM). These characteristics can be best explained by partial melt driven by a compositional change produced early in the Earth's history and a vertical thermal gradient within the layer. This boundary layer may provide an explanation for the distinctive isotope geochemical DUPAL anomaly observed at some surface ocean islands.

Keywords: thermochemical properties; boundary layer; partial melting; core–mantle boundary; Earth; differentiation

1. Introduction

Variations of chemistry inside the Earth are expected from early accretion and chemical differentiation. Identifying chemically distinct reservoirs is important not only for understanding the evolution and differentiation of the Earth, but also for studying mantle convection and geochemistry, since those chemical reservoirs are part of the Earth's circulation system [1–3] and possibly contribute to or affect geochemical signatures [4] and geodynamic observations [5] at the surface of the Earth. Despite their significance for understanding our Earth, deep chemical reservoirs remain undetected due to the challenge of distinguishing seismic effects of chemistry from those of temperature [6]. Here, we report seismic evidence for a unique 300 km thick thermo-chemical layer at the base of the mantle beneath the south Atlantic ocean. This boundary layer has steeply dipping edges, anomalously low shear wave velocities linearly decreasing from 2% (top) to 10–12% (bottom), and a maximum P velocity reduction of 3% relative to the preliminary reference Earth model (PREM) [7].

2. Seismic observations and models

Our results are based on travel time analysis and waveform modeling of transversely polarized

* Corresponding author. Tel.: +1-631-632-1726; Fax: +1-626-632-8240; E-mail: lianxing.wen@sunysb.edu

0012-821X/01/$ – see front matter
PII: S0012-821X(01)00365-X

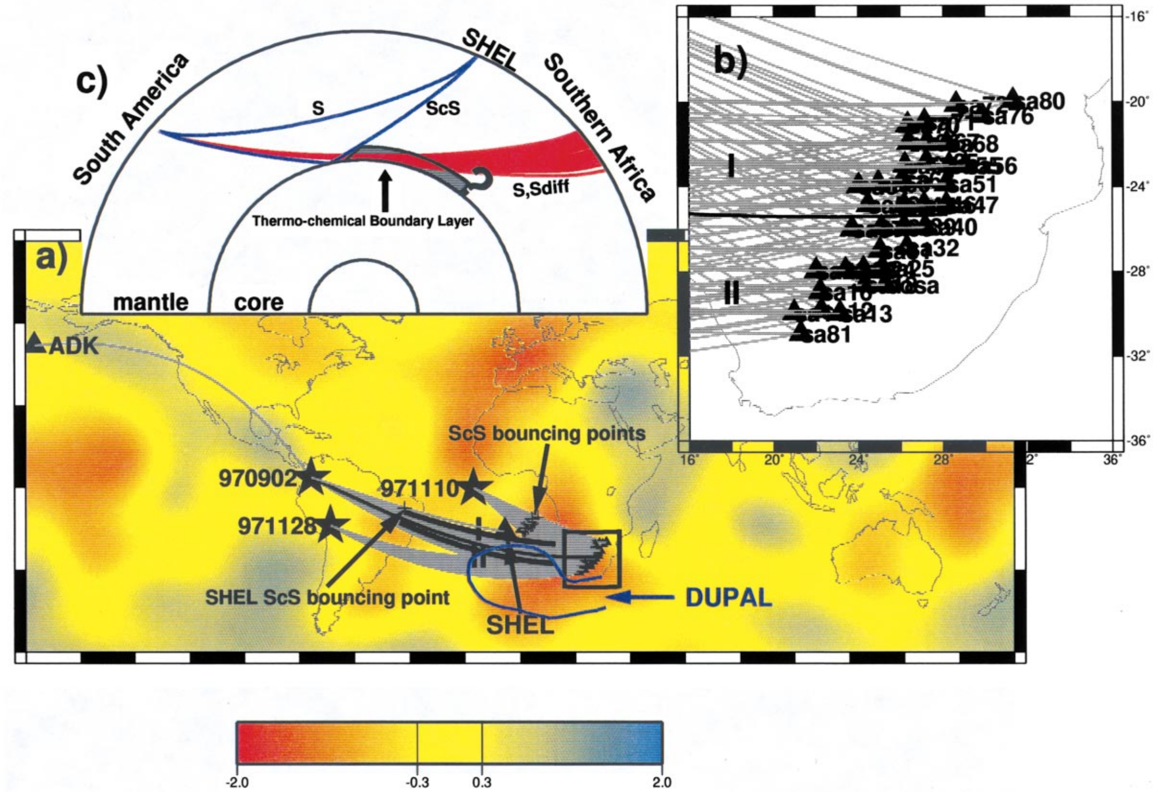

Fig. 1. (a) The great-circle paths of SH,SH_{diff} phases from three events (stars and Table 1) to the southern African array (triangles) and stations ADK, SHEL of the Global Seismic Network, along with the large scale seismic velocity structure in the lowermost mantle from Su et. al. [10] and the DUPAL anomaly maxima in the south Atlantic ocean [33–35]. The seismograms for these events are shown in Figs. 2 and 3A,B, with direct waves for event 970902 diffracting along the core–mantle boundary (Fig. 1c); those for event 971128 bottoming from the lower mantle to the core–mantle boundary; and those for event 971110 turning in the upper mantle and top of the lower mantle. The ScS bounce points at the core–mantle boundary are shown as crosses. The ScS waveforms for event 971110 are shown in Fig. 3A and that recorded at SHEL for event 970902 is shown in Fig. 2e. The moderate heavy line indicates a geographic division of the two groups, with waveforms recorded in these two groups shown in Fig. 2a,c. Two heavy lines represent two average sections at the core–mantle boundary where detailed waveform modeling is performed (Fig. 2b,d). The box indicates the southern African array (Fig. 1b). (b) The southern African array with part of the great-circle paths and the dividing line between the two groups. (c) Raypaths of SH, ScS and SH_{diff} phases as well as location and geometry of a 300 km thick layer (shaded region) with a linear reduction of shear wave velocity from 2% (top) to 10–12% (bottom). The blue (red) traces represent seismic ray paths without (with) travel time delays with respect to the predictions from the IASP 91 model.

shear waves and P waves, propagating near and along the core–mantle boundary (SH,SH_{diff} and P,P_{diff} waves, respectively). Most of our dataset consists of transverse components of displacement recorded by a dense temporary seismic array deployed in southern Africa from April 1997 to July 1999 (Fig. 1). Our dataset also includes shear wave displacements recorded in a seismic network deployed in the European–Mediterranean area and the Global Seismic Network. Because of the simplicity of the earthquake source, the ground displacements recorded across the southern African array for an earthquake in South America (970902, Fig. 1) provide a good opportunity to perform waveform modeling and travel time analysis. These observations exhibit significant complexities and variations of waveforms, as well as 10 s of direct arrival delay relative to the predictions by IASP91 [8] (Fig. 2). Most of these direct waves diffract some distance near the base of the mantle (Fig. 1c). We divide the seismograms into two groups, based on the appearance of their wave-shapes. Seismograms in groups I and II correspond to observations in the northern and southern parts of the array, respectively (see the regions and the dividing line in Fig. 1). The closest station separation between the two groups is 113 km. Note, however, different waveform complexities in the two groups (Fig. 2a,b). The waveform complexities and travel time delays are caused by anomalous seismic structures in the lowermost 300 km of the mantle, as other possible causes can be confidently eliminated. (1) They cannot be the result of hypocenter mislocation or seismic heterogeneities in the source-side mantle. As the observed SH phases propagate over almost identical raypaths in the source-side mantle, mislocation and heterogeneities in the source-side mantle should result in similar time delays and waveforms across the array. (2) The waveform complexities cannot be caused by a complicated earthquake source for two reasons: (a) the waveform complexities in the two groups are markedly different; and (b) the waveform observed at station ADK, which samples a different path through the mantle, displays a simple pulse-like shape (Fig. 2a), indicating a simple source time function. (3) Near-station effects and upper mantle structure appear to contribute little to the observed time delays across the seismic array. In

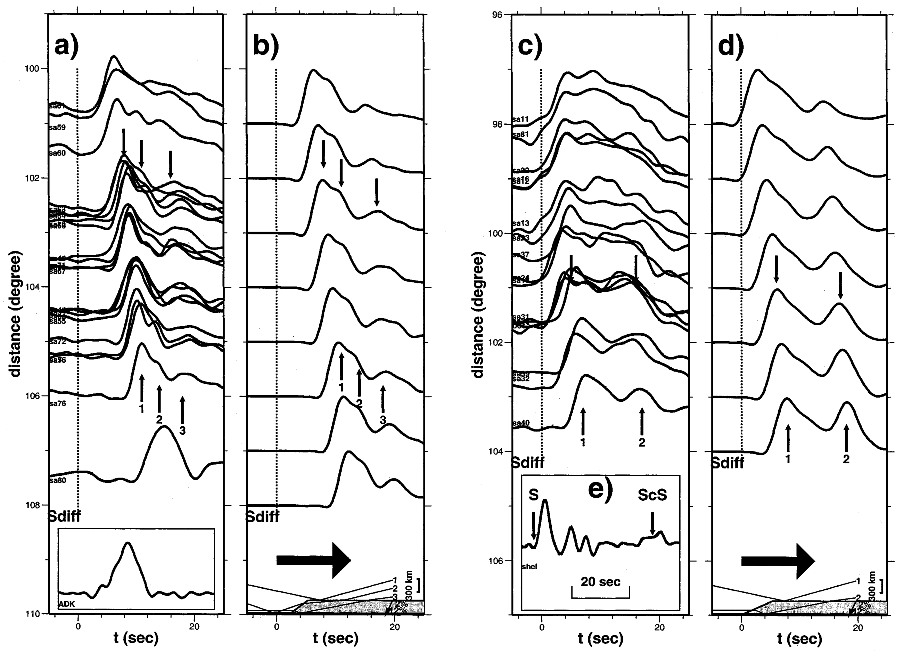

Fig. 2. Transverse components of displacement of group I (a) and group II (c) for event 970902 recorded at the southern African array as well as corresponding synthetic seismograms (b, d) calculated using models of a 300 km thick layer at the bottom of the mantle with a linear decrease of shear wave velocity from 2% (top) to 12% (bottom) relative to PREM [7] (see Fig. 1 for the great-circle paths and the geographic division between the two groups; and Fig. 4 for seismic models). Each trace is aligned along the theoretical predicted arrival of the SH_{diff} phase (dashed lines labeled S_{diff}). The raypaths associated each individual phase are labeled and schematically shown at the bottom of (b) and (d) and Fig. 4. The directions of wave propagation are indicated by the horizontal arrows. A record observed at station ADK (Fig. 1) is displayed at the bottom of (a), indicating a simple source time function for this event. A record observed at station SHEL is displayed in (e), with arrows indicating the predicted arrivals of S and ScS phases by PREM (see Fig. 1 for the ScS bounce point). Note the time delays and waveform complexities across the array, and the waveform differences between the two groups. Note also the sensitivity of synthetic waveforms to the edge dips.

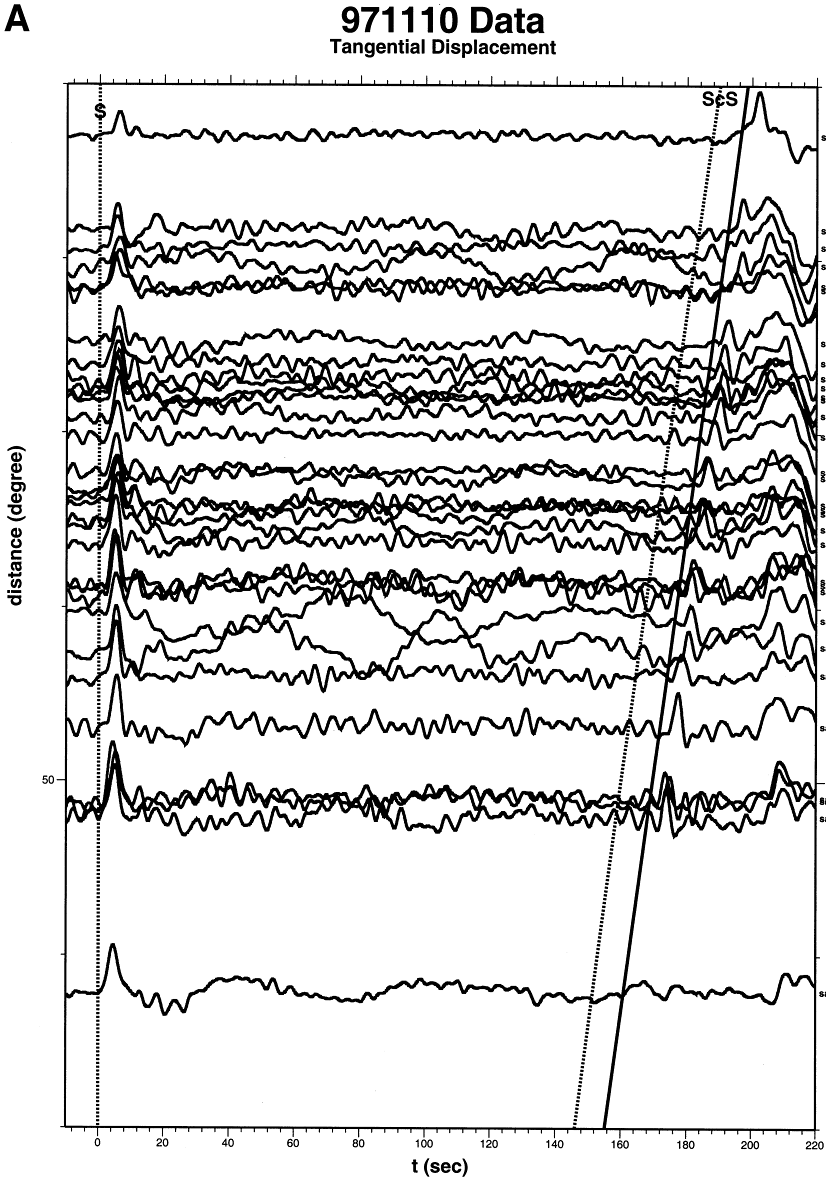

Fig. 3. Transverse components of displacement for events 971110 (A) and 971128 (B) recorded on the southern African array. Traces are aligned along their theoretical predicted direct SH arrivals (dash lines labeled as S) based on IASP91 [8]. In (A), the heavy line is the predicted ScS travel time from a uniform 300 km thick layer at the bottom of mantle with a linear decrease of shear wave velocity from 2% (top) to 12% (bottom), i.e., the velocity structures of the anomalous layer shown in Fig. 2b,d. In (B), seismograms with their direct waves turning 300 km above the core–mantle boundary are displayed as light traces, whereas those with their direct waves turning within 300 km of the lowermost mantle are shown in heavy lines. Note that systematic time delays are only observed for those direct SH waves turning within the lowermost 300 km of the mantle. Note also the large time delays for ScS phases (cf., theoretical predicted arrivals labeled as ScS) observed at all stations. These figures demonstrate that station effects and seismic structures in the upper mantle and the mid-lower mantle contribute little to the observed travel time delays and waveform complexities for event 970902.

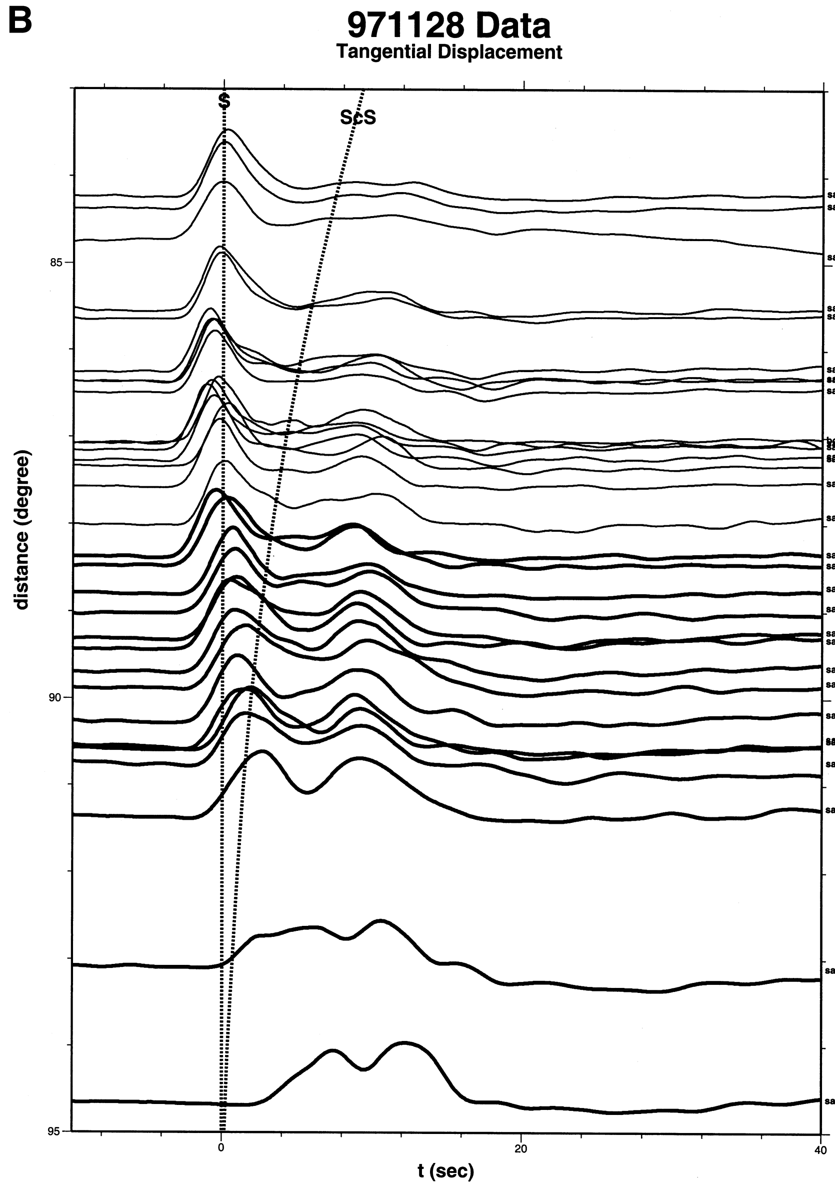

Fig. 3 (*continued*).

particular, direct SH waves recorded by event 971110, which sample the upper mantle and top of the lower mantle, show little time variation across the seismic array (Fig. 3A). Significant travel time delays are observed, however, for the core-reflected ScS phases (Fig. 3A). (4) Finally, the complexities and large time delays are not caused by seismic structures in the mid-lower mantle, since the SH phases bottoming more than 300 km above the core–mantle boundary from event 971128 (Fig. 3B, light traces), exhibit simple waveforms and little residual time variations across the array. These phases and the direct SH_{diff} phases sample a similar receiver-side mid-lower mantle. For event 971128, however, large systematic time delays are observed for the SH

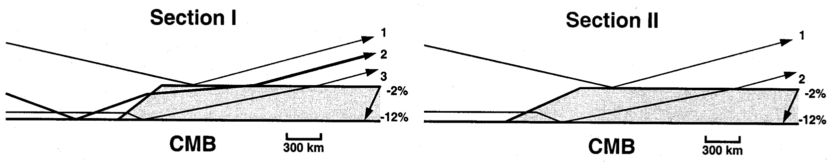

Fig. 4. Seismic models for two cross-sections (see Fig. 1 for geographic locations; heavy lines labeled as I and II) near the core–mantle boundary. The synthetic seismograms predicted based on these two models are shown in Fig. 2b (section I) and Fig. 2d (section II). Both models have a thickness of 300 km and a linear decrease of shear wave velocity from 2% (top) to 12% (bottom) relative to PREM. The raypaths associated with each individual phase in Fig. 2b,d are schematically shown.

phases turning in the lowermost 300 km of the mantle (Fig. 3B, heavy traces), as well as for the ScS phases recorded at all stations, suggesting a shear velocity anomaly starting at 300 km above the core–mantle boundary.

The timing of direct and late arrivals and the complexities of observed waveforms suggest that the seismic waves encounter three-dimensional structure in the lowermost 300 km of the mantle. Waveforms of the observed SH phases are sensitive to the seismic velocity variations and laterally dipping structures in the lowermost mantle, where these phases propagate horizontally. In general, a more steeply dipping edge structure produces a stronger first arrival relative to its multiples and a shorter time separation between them; and different vertical velocity gradients generate different move-outs of multiples, different amplitude ratios between the first arrival and multiples, and different frequency contents of the first arrivals. Computed synthetic seismograms confirm the sensitivity of waveforms to these seismic parameters. Among the series of models with different seismic parameters, the most successful models for the two groups of observations involve a 300 km thick layer with an abrupt velocity decrease of 2% at the top, a linear decrease of velocity to 10–12% at the core–mantle boundary, and steeply dipping boundaries at the edge (26–38°) (Fig. 4). Only a slight change in edge dip is required to match the observations in the two groups (Figs. 2 and 4). The travel times of direct SH waves constrain the thickness of the anomalous layer, corroborated well by the observations in event 971128 (Fig. 3B). The existence of multi-path phases (labeled as 2, Fig. 2b) and multiples inside the layer (labeled as 3, Fig. 2b; labeled as 2, Fig. 2d) place tight constraints on the edge dip, the magnitude of velocity reductions, and the vertical velocity gradient. The seismic technique and the detailed modeling will be presented in a separate paper [9]. We present some examples of synthetic seismograms to illustrate the sensitivity of model parameters to seismic wave propagation (Fig. 5). The phase 2 observed in Fig. 2a requires layers with: (1) a large negative velocity gradient ($>9\%$), a certain thickness (>250 km) and steeply dipping edges. Note that all these models in Fig. 5 fail to generate the triplicated phase 2. The only models which can explain the observed travel time anomalies are 300 km thick layers with large velocity reductions. Note that a 200 km thick layer with a negative velocity gradient of 20% (Fig. 5c) and a 300 km thick layer with a negative velocity gradient of 3% cannot explain the observed travel time anomalies (Fig. 5d). Models with a negative velocity gradient of 3% embedded with a ultra-low velocity layer also predict a pulse-like first arrival and many multiples inside the layer, inconsistent with the observed waveform features (Fig. 5d). Overall, synthetics predicted by our simple models match the observations well. We nevertheless note the three-dimensional effects of wave propagation, as not all waveform variations can be explained by our models.

The geographic variation of the seismic structure is also well corroborated by the ScS phases observed at the southern African seismic array for event 971110 and at station SHEL for event 970902. The ScS travel times are well predicted on the basis of the seismic velocity structures inside (Fig. 3A) and outside the anomalous core–mantle boundary layer (Fig. 2e). Moreover, the

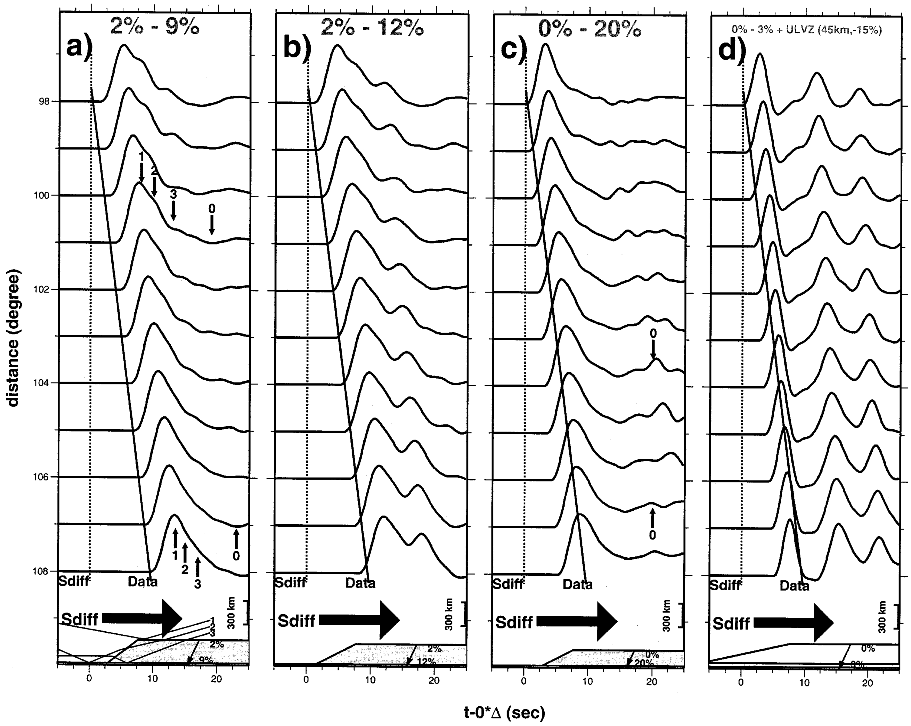

Fig. 5. Synthetic seismograms for four models selected to illustrate the sensitivity of the model parameters. (a) a 300 km thick layer with shear velocities linearly decreasing from 2% (top) to 9% (bottom); (b) a 250 km thick layer with shear velocity velocities linearly decreasing from 2% (top) to 12% (bottom); (c) a 200 km thick layer with shear velocities linearly decreasing from 0% (top) to 20% (bottom); (d) a 300 thick layer with shear velocities linearly decreasing from 0% (top) to 3% (bottom), embedded with a ultra-low velocity layer with shear velocity reduction of 15%. All traces are aligned along their theoretical predicted arrival times (dash lines, labeled as S_{diff}) and the observed travel times are shown by heavy lines (labeled as Data). The phase 0 is a truncation phase of the calculations.

S,S_{diff} displacements recorded in the European–Mediterranean region for earthquakes in the south Atlantic ridge and the south Sandwich islands show the same behavior of travel time as those recorded by the southern African array (Fig. 6A and cf., Fig. 2a,c). These observations show a linear travel time delay of up to 10 s for seismic waves turning within the lowermost

Table 1
Event list

No.	Origin	Latitude	Longitude	Depth (km)
921121	92/11/21 22:39:35	−56.66	−26.55	33
930929	93/09/29 18:26:20	−42.57	−18.43	10
950707	95/07/07 10:40:04	−53.56	9.19	10
950818	95/08/18 02:16:26	−55.90	−28.90	36
970902	97/09/02 12:13:23	3.85	−75.75	199
971110	97/11/10 12:47:34	0.05	−16.893	10
971128	97/11/28 22:53:42	−13.74	−68.79	586
971227	97/12/27 20:11:01	−55.78	−4.22	10
980624	98/06/24 10:44:31	−37.29	−17.39	10

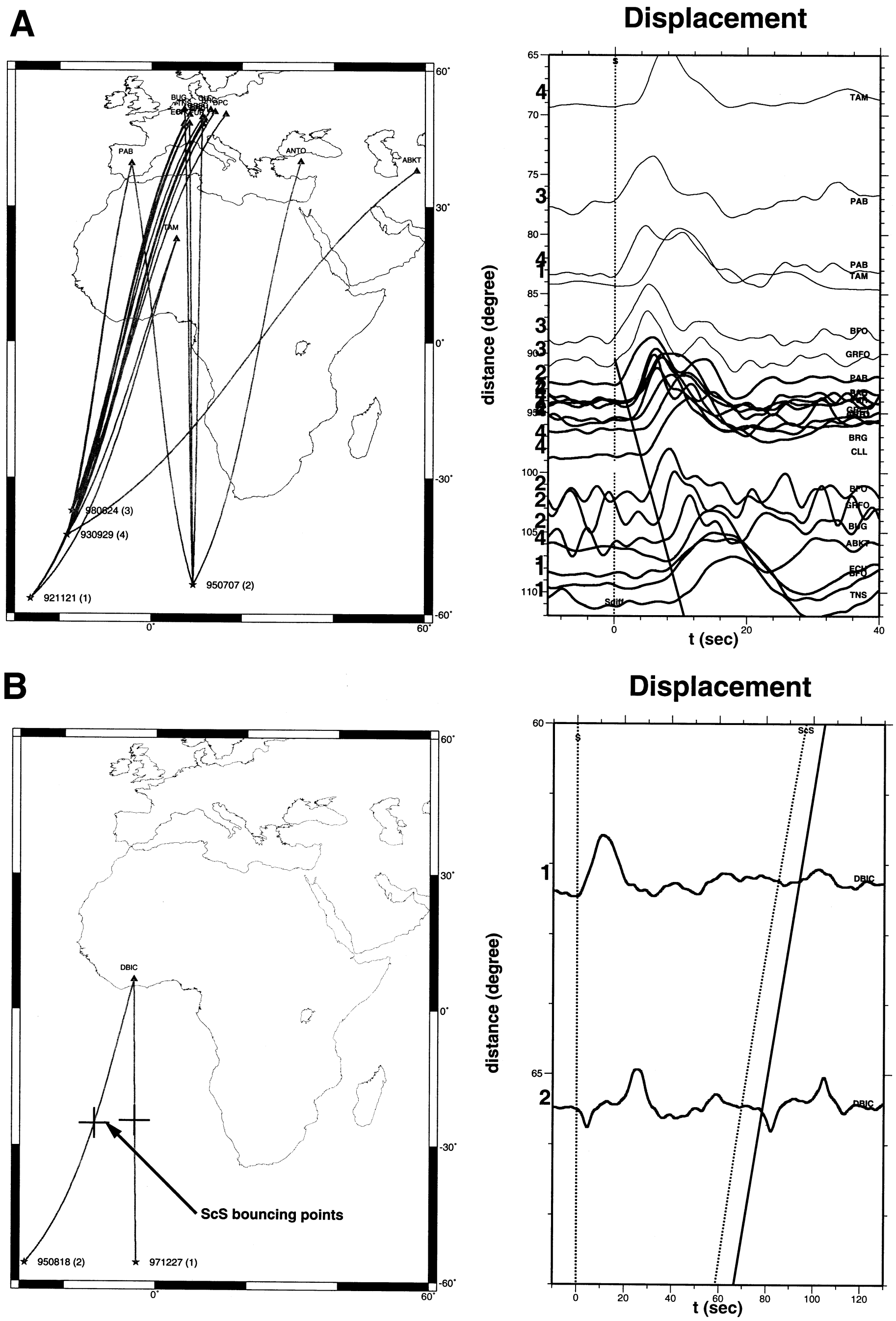

300 km of the mantle (heavy traces, Fig. 6A) and little travel time anomaly for S waves turning 300 km above the core–mantle boundary (light traces, Fig. 6A). The ScS and S phases observed at station DBIC for earthquakes in the south Sandwich Island region also show the same differential travel times as those recorded in the southern African array (Fig. 6B and cf., Fig. 3A). All these travel

Fig. 6. (A) Observed S,S_{diff} phases (right) in the European–Mediterranean region for earthquakes occurred in the south Atlantic ocean and the south Sandwich islands (left and Table 1). These traces are aligned with respect to the predicted arrivals based on the IASP 91 model after the event corrections. For each event, event correction is made by shifting all seismograms recorded for that particular event by a constant time so that the time residual for the observation at station PAB is zero with respect to the prediction by the IASP 91 model (most part of this event correction is for source depths, which are not well constrained for shallow earthquakes in the earthquake catalogs). PAB was not available for event 1. The event correction for event 1 is made by shifting the seismograms observed in event 1 by a constant time so that the time residual observed at station TAM is the same as that observed for event 4 after event 4 correction (this station effect is also observed at closer distance ranges). TAM was not available for event 2 and event 3. The light traces are for S waves turning 300 km above the core–mantle boundary and the heavy traces are for those turning the lowermost 300 km of the mantle. The event numbers are labeled in both panels. (B) Observed S and ScS phases (right) at station DBIC for earthquakes occurred in south Sandwich island (left and Table 1). Traces are aligned on the S arrivals ($t = 0$). The dash lines are theoretical predicted arrivals for S and ScS phases based on the IASP 91 model. The event numbers are labeled in both panels.
←

time anomalies are exactly predicted by our models. Geographically, the seismic waves recorded in the European–Mediterranean region (Fig. 6A,B) and those recorded in the southern Africa (Figs. 2a,c and 3A,B) sample the same region of the

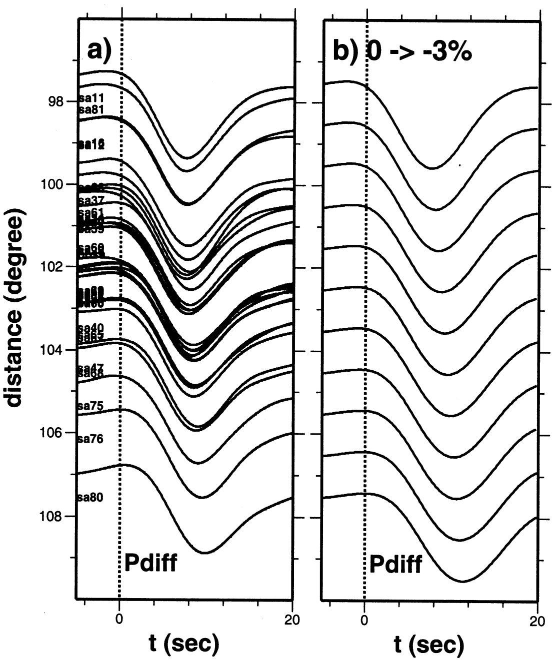

Fig. 7. Vertical component of displacement recorded in the southern African array for event 970902 (left panel) and synthetic seismograms (right panel) calculated using a model with compressional velocity decreases from 0% (top) of 3% (bottom) across the 300 km thick layer. The model geometry is the same as those in Fig. 2. Note that predicted travel time delays are slightly larger than those observed. Thus these compressional velocities should be considered as the upper bound.

lowermost mantle, but different parts of the mid-lower mantle. These observations affirm our conclusion that both the travel time anomalies and the waveform complexities observed in the southern African array for event 970902 (Fig. 2a,c) are caused by anomalous seismic structures in the lowermost 300 km of the mantle.

The travel time variation of the compressional P,P_{diff} phases recorded for event 970902 can be used to place bounds on the P velocity gradient across the boundary layer. A maximum compressional velocity decrease of 3% across the anomalous layer is found from modeling the observed compressional waves (Fig. 7). As we discussed before, the travel time variation across the array would not be affected by seismic structures in the source-side mantle and earthquake mislocation. The estimate of this upper bound will not be affected by the seismic structures in the receiver-side mantle either, because the seismic velocity anomaly in the receiver-side mantle, even if it exists, would likely have slower than average velocities.

3. Interpretations

It has always been difficult and ambiguous to interpret seismic structures in the deep mantle due to the challenge of distinguishing seismic effects of chemistry from those of temperature [6]. As we have shown above, the waveform features recorded in the southern African array enable us to constrain the seismic parameters which are crucial to interpreting the seismic structures, such as geometry, magnitude, and detailed distribution of seismic velocities. The dense coverage of phase pairs of S,S_{diff} and P,P_{diff} also enables us to constrain the ratio of shear wave to compressional wave velocity perturbations ($\partial \ln V_s/\partial \ln V_p$). The existence and uniqueness of these anomalous seismic characteristics (magnitude, geometry and $\partial \ln V_s/\partial \ln V_p$) should hold the key to pinning down the most plausible origin of this anomalous boundary layer through a comparative study with other regions of the core–mantle boundary. We discuss the possible interpretations in the framework of an isochemical mantle and a chemically heterogeneous mantle.

For an isochemical mantle, the magnitude of shear wave velocity perturbations requires an unreasonable temperature elevation by about 2500–3500 K across the boundary layer [11], so partial melt is required to explain the magnitude of those perturbations [12]. The most likely scenario is that some mineral component (e.g., magnesiowüstite) starts to melt at 300 km above the core–mantle boundary, as the mantle geotherm intersects the eutectic melting temperature of mantle composition. The difficulty of this interpretation lies in explaining the geometry of the observed anomalous structure and comparing with seismic structures in other regions of the core–mantle boundary. As $\partial T_m/\partial P$ is small because of the small volume change ΔV at high pressures ($\partial T_m/\partial P = \Delta V/\Delta S$, T_m is solidus temperature, P is pressure and ΔS is the change of entropy), the onset of partial melt approximately represents an isotherm in the mantle. Mantle flow would unlikely generate an isotherm with the abrupt changing geometry shown in Fig. 4. Partial melting in an isochemical mantle also encounters difficulties in explaining seismic structures in the lowermost mantle globally. As the core–mantle boundary is presumably an isotherm because of the likely absence of lateral temperature gradients in the outer core [13], this partially molten layer should occur globally with its thickness modulated by mantle flow. No evidence for the global existence of such a layer has been reported. Ultra-low velocity zones are reported elsewhere, but the evidence for their existence has been limited to some localized regions from SKS-SPdKS phase [14–16] and PKP precursors [17–20]. Moreover, the vertical scales of ultra-low velocity zones are on the order of just 5–40 km [14–20]. The African anomalous layer is also dramatically different from the seismic structure beneath the central Pacific, where a similar condition of mantle temperature may be expected. There, however, a shear wave velocity decrease of only 3% is observed at the bottom of the mantle [9,21–22]. It is thus clear that the anomalous layer cannot readily be explained within the framework of an isochemical mantle.

For a chemically heterogeneous mantle, a chemical anomaly produced by core–mantle reaction or segregation of subducted oceanic crust would not likely explain the unique presence and the steeply dipping edges of this anomalous layer. The following chemical reactions between core iron alloys and mantle silicates have been proposed [23]:

$$(\mathrm{Mg}_x,\ \mathrm{Fe}_{1-x})\mathrm{SiO_3} + 3[(1-x)-s]\mathrm{Fe} = x\mathrm{MgSiO_3} + \mathrm{sSiO_2} + [(1-\mathrm{x})-\mathrm{s}]\mathrm{FeSi} + [3(1-\mathrm{x})-2\mathrm{s}]\mathrm{FeO} \quad (1)$$

where $1-x$ is the amount of iron in reacting mantle material, and s is the amount of silica generated by the reaction. A thin boundary layer would be expected as a result of slow chemical diffusion [24]. Background mantle flow, however, may accelerate the diffusion process by entraining the material upward [25]. Some reactant products may lower the melting temperatures of mantle solids and cause partial melt, which may also provide positive feedback to these chemical reactions [26]. So it is difficult to evaluate the change of seismic properties as a result of these reactions. But one would expect a shallow dip at the edge of the layer [25], a complex internal structure and the existence of similar structures in some other regions (e.g., the central Pacific) as a result of background mantle flow. It also requires special pleading to envision that oceanic crust could accumulate to a 300 km thick layer, and preferentially melts and resides in one particular region of the core–mantle boundary. Numerical studies of mantle convection also indicate that a large portion of the oceanic crust would mix back into the mantle and that the edge of the segregated oceanic crust would be more gradually sloping than what is shown from our models (Fig. 4) [27].

We suggest that a localized chemical anomaly produced by the early Earth's differentiation would be more consistent with the observed seismic structure. Melting and gravitational separation are likely the dominant processes in the Earth's chemical differentiation. Just as the Earth's surface has preferentially segregated less dense chemical bodies (e.g., continents) from the buoyant melts, the chemical boundaries in the deep mantle may be preferentially enriched in dense phases (cf., the core-formation process). The core–mantle boundary is evidently one of the most plausible deep repositories for dense materials due to the large density difference across the boundary. When the Earth was a completely or partially molten body to great depth in its early history [28], some dense (e.g., iron-enriched) melts in the mantle could reach the core–mantle boundary by direct sinking, percolation through perovskite solid matrix [29,30], or an avalanche of a dense layer at the top of the lower mantle [31].

Not only does a primordial differentiation mechanism readily explain the steeply dipping edges and the unique presence of the anomalous layer, but also it provides a feasible physical mechanism for the localized partial melting. The following two characteristics of such a chemical anomaly should significantly affect its melting behavior: (1) it may be enriched in less compatible elements (e.g., Al, Fe, Ca) and perhaps some volatile components. Although these elements are probably minor, they could significantly depress the melting temperature locally; (2) it may also be enriched in heat producing incompatible elements, such as U, Th, K. Internal temperature may be so elevated due to radiogenic heating that it sustains the partial melting or re-melts locally. For a reference, for materials with chondrite heating rate [32], 5.2×10^{-12} W/kg, temperature will increase about 130°K in 1 Gyr. In this partial melt scenario, melting at a chemical boundary or at the eutectic temperature results in an abrupt decrease of velocity at 300 km above the core–mantle boundary, and an increase of both melt fraction and temperature produces a negative velocity gradient toward the core–mantle boundary.

4. Possible implications

If the deep mantle structure we observed is indeed 'an ancient enriched anomaly' formed in the early Earth's history, it could shed light on many other aspects of the Earth's dynamics. Some islands in the south Atlantic and Indian oceans have distinct enriched isotope geochemistry [33–35] and coincide with the areal extent of the anomalous seismic layer at the core–mantle boundary (Fig. 1). The isotope data indicate that this isotope geochemistry is related to very early (>3 Gyr) development of enrichment of incompatible elements [33–35]. This anomalous seismic layer may provide an explanation for the observed distinctive enriched isotope geochemistry, if mantle flow is able to entrain the anomalous materials and carry them to the Earth's surface.

The existence of chemical heterogeneities produced in the early Earth's differentiation processes may also provide an explanation for the proposed partial melt for the ultra-low velocity zones near the core–mantle boundary [12]. The ultra-low velocity zones observed in other regions [14–20] may just reflect the existence of these chemical heterogeneities in different length scales and with different degrees of partial melt.

5. Conclusions

We report seismic observations of S, ScS, S_{diff}, P, P_{diff} phases sampling the lowermost mantle beneath the south Atlantic ocean. Both the S,S_{diff} phases recorded in the Kaapvaal seismic array for earthquakes in the South American subduction zone and those recorded in the European–Mediterranean area for earthquakes in the south Sandwich islands exhibit a linear delay of 10 s for the seismic waves bottoming the lowermost 300 km of the mantle (to an epicentral distance of 108°) and little travel time delay for the seismic waves turning 300 km above the core–mantle boundary. Those recorded at the diffracted distance range of 98–108° in the Kaapvaal seismic array also show discernible multiple ScS phases with the same slowness as the direct SH waves up to

108° and rapid variations of waveform across small epicentral distances, and those recorded at a closer distance range of 83–95° show large *ScS*–*S* time separations and a rapid increase of *ScS* amplitude. P_{diff} phases recorded in the Kaapvaal seismic array for the same earthquakes, on the other hand, show little travel time delays across the seismic array.

Both the observed travel times and waveform features suggest a 300 km thick layer at the base of the mantle beneath the south Atlantic ocean, with a steeply dipping edge, anomalously low shear wave velocities linearly decreasing from 2% (top) to 10–12% (bottom), and a maximum P velocity reduction of 3% relative to the (PREM). These characteristics can be best explained by partial melt driven by a compositional change produced early in the Earth's history and a vertical thermal gradient within the layer. This boundary layer may provide an explanation for the distinctive isotope geochemical DUPAL anomaly observed at some surface ocean islands.

Acknowledgements

The seismic data used in this paper were collected as part of the Kaapvaal research project. The project is funded by the National Science Foundation's Continental Dynamics program and by agencies in southern Africa. Principal academic collaborators include Carnegie Institution and MIT in the United States and the University of Cape Town, the University of the Witwatersrand, the University of Botswana and the Botswana Geological Survey, and the University of Zimbabwe in southern Africa. Exploration companies Anglo American, de Beers, BHP, and Rio Tinto, Zimbabwe provided invaluable logistical and intellectual resources for the experiment. Four service groups maintained the stations and collected data in the field: U. Capetown (with BHP), Kimberley (de Beers), U. Witwatersrand, and U. Zimbabwe (with Rio Tinto). Special thanks go to Dr. Rod Green for invaluable contributions to the field program. Thanks also to Sue Webb, Jock Robey, Eddie Kostlin, Maggie Jutz and all the members of the Kaapvaal Seismic Group for major contributions to the success of the project. A full list of participants can be found at http://www.ciw.edu/kaapvaal. Yingwei Fei provided us assistance in understanding mineral physics. Don Anderson, Steve Grand, and an anonymous reviewer provided critical reviews and comments, which improved the paper significantly. We also thank Donald Helmberger, David Stevenson, Ron Cohen, Sean Solomon, Donald Weidner, Bob Libermann and Bill Holt for stimulating discussions and reviews. Most of this work was done when L.W. was at Carnegie Institution of Washington. This work is supported by a fellowship at Carnegie Institution of Washington and an NSF Grant EAR0001232.***[RV]***

References

[1] G.F. Davies, Geophysical and isotopic constraints on mantle convection: an interim synthesis, J. Geophys. Res. 89 (1984) 6017–6040.
[2] L. Wen, D.L. Anderson, Present-day plate motion constraint on mantle rheology and convection, J. Geophys. Res. 102 (1997) 24639–24654.
[3] P.J. Tackley, Three-dimensional simulations of mantle convection with a thermo-chemical basal boundary layer:D″? in: M. Gurnis, M.E. Wysession, E. Knittle, B. Buffet (Eds.), The Core–mantle Boundary Region, Vol. 28, Geodynamics, American Geophysical Union, Washington, DC, 1998, pp. 231–253.
[4] A.W. Hofmann, Mantle geochemistry the message from oceanic volcanism, Nature 385 (1997) 219–228.
[5] B.H. Hager, R.W. Clayton, Constraints on the structure of mantle convection using seismic observations, flow models, and the geoid, in W.R. Peltier (Ed.), Mantle Convection, Gordon and Breach, Newark, NJ, 1989, pp. 657–764.
[6] T. Lay, Q. Williams, E.J. Garnero, The core–mantle boundary layer and deep Earth's dynamics, Nature 392 (1998) 461–468.
[7] A. Dziewonski, D.L. Anderson, Preliminary reference Earth model, Phys. Earth Planet. Inter. 25 (1981) 297–395.
[8] B.L.N. Kennett, IASP 91, Australian National University, Canberra, 1991.
[9] L. Wen, An SH hybrid method and shear velocity structures in the lowermost mantle beneath the central Pacific and South Atlantic oceans, J. Geophys. Res., submitted, 2001.
[10] W.J. Su, R.L. Woodward, A.M. Dziewonski, Degree 12 model of shear velocity heterogeneity in the mantle, J. Geophys. Res. 99 (1992) 6945–6980.

[11] Y. Wang, D.J. Weidner, $(\partial\mu/\partial T)_p$ of the lower mantle, Pure Appl. Geophys. 146 (1996) 533–549.
[12] Q. Williams, E.J. Garnero, Seismic evidence for partial melt at the base of Earth's mantle, Science 273 (1996) 1528–1530.
[13] D.J. Stevenson, Limits on lateral density and velocity variations in the Earth's outer core, Geophys. J. R. Astron. Soc. 89 (1987) 311–319.
[14] E.J. Garnero, S.P. Grand, D.V. Helmberger, Low P-wave velocity at the base of the mantle, Geophys. Res. Lett. 23 (1993) 977–980.
[15] L. Wen, D.V. Helmberger, A two-dimensional P–SV hybrid method and its application to modeling localized structures near the core–mantle boundary, J. Geophys. Res. 103 (1998) 17901–17918.
[16] D.V. Helmberger, L. Wen, X. Ding, Seismic evidence that the source of Iceland hotspot lies at the core–mantle boundary, Nature 396 (1998) 251–255.
[17] L. Wen, D.V. Helmberger, Ultra low velocity zones near the core–mantle boundary from broadband PKP precursors, Science 279 (1998) 1701–1703.
[18] J.E. Vidale, M.A. Hedlin, Intense scattering at the core–mantle boundary north of Tonga: Evidence for partial melt, Nature 391 (1998) 682–684.
[19] L. Wen, D.V. Helmberger, Global behavior of PKP precursors and seismic scattering in the lowermost mantle, EOS 80 (1999) S217.
[20] L. Wen, Intense seismic scattering near the Earth's core–mantle boundary beneath the Comoros hotspot, Geophys. Res. Lett. 27 (2000) 3627.
[21] J. Ritsema, E.J. Garnero, T. Lay, A Strongly negative shear velocity gradient and lateral variability in the lowermost mantle beneath the Pacific, J. Geophys. Res. 102 (1997) 20395–20411.
[22] M.E. Wysession, A. Langenhorst, M. Fouch, K.W. Fischer, G.I. Al-Eqabi, P.J. Shore, T.J. Clark, Lateral variations in compressional/shear velocities at the base of the mantle, Science 284 (1999) 120–125.
[23] E. Knittle, R. Jeanloz, Earth's core–mantle boundary results of experiments at high pressures and temperatures, Science 251 (1991) 1438–1443.
[24] D.J. Stevenson, Why D″ is unlikely to be caused by core–mantle interactions, Eos 74, 1993, 51 pp.
[25] L.H. Kellogg, S.D. King, Effect of mantle plumes on the growth of D″ by reaction between the core and mantle, Geophys. Res. Lett. 20 (1993) 379–382.
[26] R. Jeanloz, Q. Williams, The core–mantle boundary region, in: R.J. Hemley (Ed.), Ultrahigh-pressure mineralogy, Mineralogical Society of American, Washington, DC 37, 1998, pp. 241–259.
[27] U.R. Christensen, A.W. Hofmann, Segregation of subducted oceanic crust in the convecting mantle, J. Geophys. Res. 99 (1994) 19867.
[28] G.W. Wethrill, Occurrence of giant impacts during the growth of terrestrial planet, Science 228 (1985) 877–879.
[29] S. Urukawa, M. Kato, M. Kumazawa, Experimental study on the phase relations in system Fe–Ni–O–S up to 15 GPa, in: M. Manghnani, Y. Syono (Eds.), High Pressure Research in Mineral Physics, American Geophysical Union, Washington, DC, 1987, pp. 95–111.
[30] D.J. Stevenson, Fluid dynamics of core formation, in: H.E. Newsom, J.H. Jones (Eds.), Origin of the Earth, Oxford University Press, New York, 1990, pp. 231–249.
[31] P.J. Tackley, D.J. Stevenson, G.A. Glatzmaier, G. Schubert, Effects of an endothermic phase transition at 670 km depth in a spherical model of convection in the Earth's mantle, Nature 361 (1993) 699–704.
[32] F.D. Stacy, Physics of the Earth, Brookfield, Kenmore, Qld, 1992.
[33] B. Dupre, C.J. Allègre, Pb–Sr isotope variation in Indian Ocean basalts and mixing phenomena, Nature 303 (1983) 142–146.
[34] S.R. Hart, A large-scale isotope anomaly in the Southern Hemisphere mantle, Nature 309 (1984) 753–757.
[35] S.R. Hart, Heterogeneous mantle domains: signatures, genesis and mixing chronologies, Earth Planet. Sci. Lett. 90 (1988) 273–296.